Module 7 - Optical sources and transmitter

Dr. Alan Kost

Associate Research Professor of Optical Sciences, University of Arizona

Dr. Alan Kost is an Associate Research Professor of Optical Sciences in the University of Arizona. His areas of research include optical data storage, optical communications, integrated optics, nano-optics.

Email: akost@arizona.edu

Introduction

The following module continues the discussion of optical sources for telecommunications systems and networks.   Particular designs concerns based on source profile, output and efficiency are treated and issues of transmitter circuitry and packaging design are discussed.

7.1 Source Design Concerns
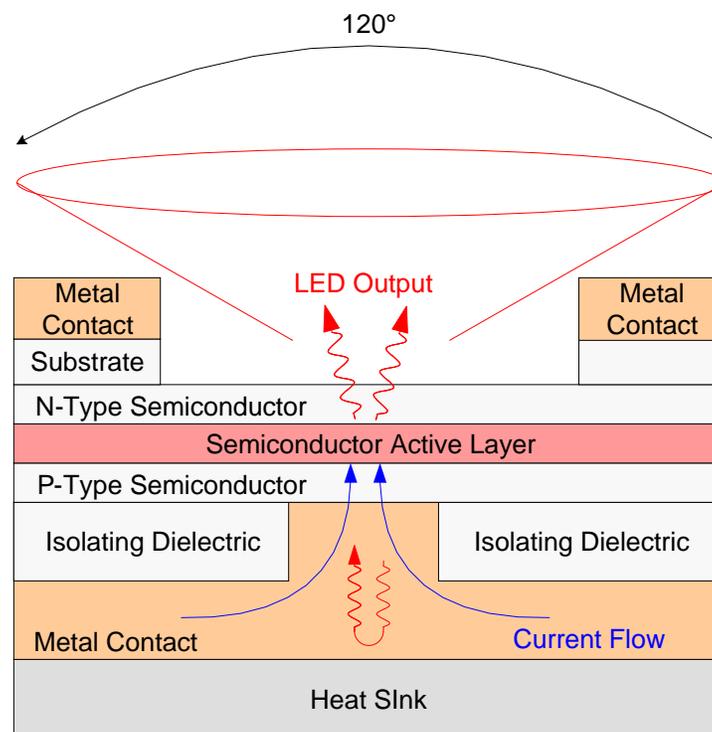
Laser Mode Profile

Figure 7.1: *The output of a light emitting diode is an isotropic Lambertian pattern.*

Emission from light emitting diodes (LEDs) is isotropic and Lambertian-like. The internal emission is in all directions, but total internal reflection at the surface of the semiconductor limits the light that escapes an LED to a cone with a full width at half maximum (FWHM) angle of approximately 120 degrees. A Lambertian source is a source whose radiance (or power per unit area per unit solid angle) is constant in all directions.

The output profile of an edge emitting semiconductor laser is considerably narrower than for a light emitting diode. The output is shaped into a beam by the mirrors that form the laser resonator. The far-field output profile is asymmetric with a full width at half maximum angle of 5-10 degrees in the horizontal "slow axis" direction and a full width at half maximum angle of 30-50 degrees in the vertical "fast axis" direction. The angular profile of the beam is often approximated by a Gaussian.
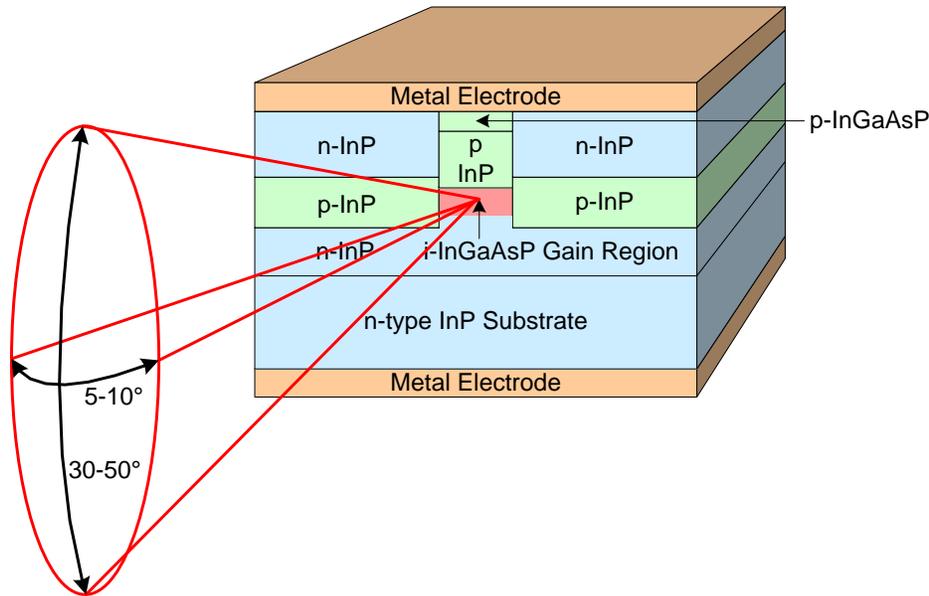

Figure 7.2: *The far-field output beam profile for an edge emitting semiconductor laser.*

Vertical cavity surface emitting lasers, or VCSELs, have a disk shaped gain medium and a fundamental lateral mode with a far field output that is Gaussian and rotationally symmetric about the direction of beam propagation. The divergence angle of the far field beam depends on the beam spot size in the gain medium; however, a typical spot size of approximately 6 microns in diameter results in a divergence angle of approximately 6 degrees (FWHM).
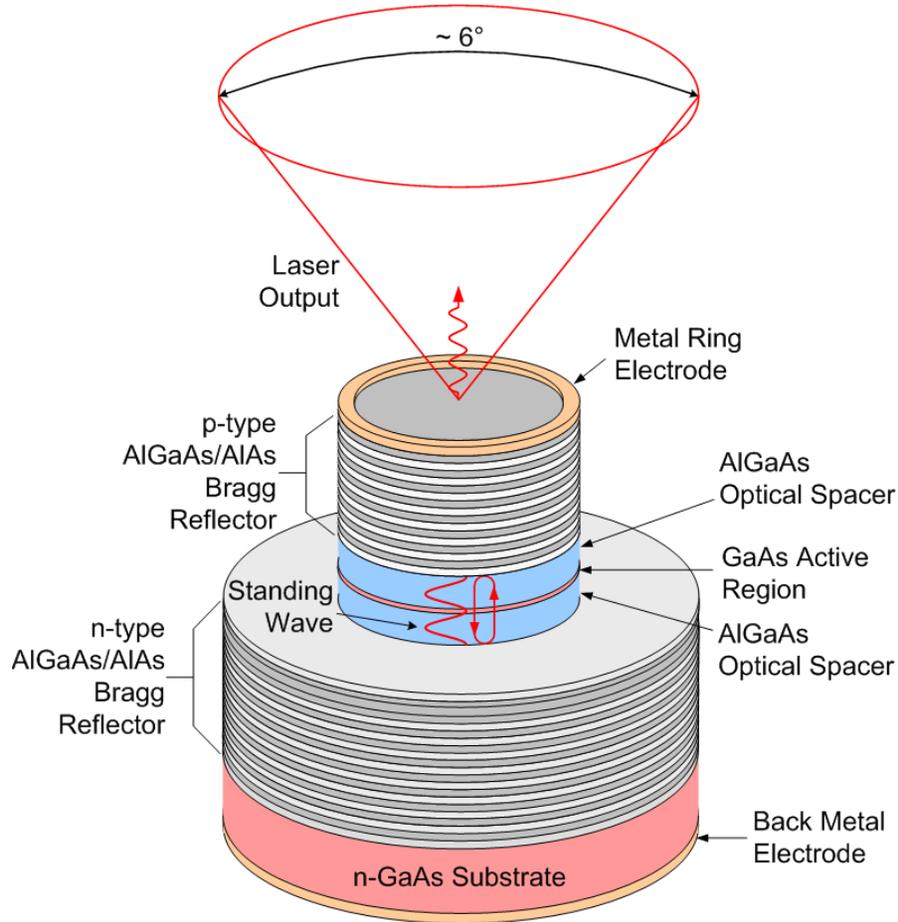
Figure 7.3: *The far-field output profile for a vertical cavity surface emitting laser.*

Output Power

The output of a light emitting diode (LED) is both temporally and spatially incoherent. The output power of a typical light emitting diode is on the order of 30 mW with a pump current of 40 mA.

The coherent optical output of an edge emitting laser is characterized by a light-current, or L-I, curve. The L-I curves for a buried heterostructure laser at various temperatures are shown in **Figure 7.4**.
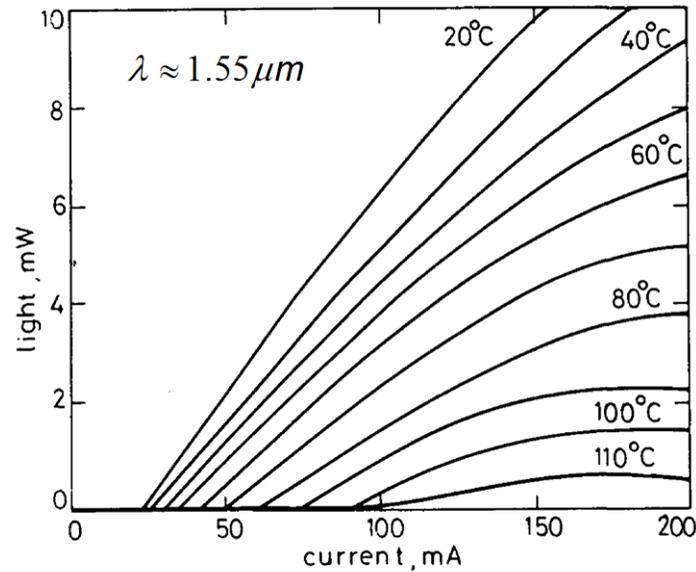
Figure 7.4: *Light versus current curves for a buried heterostructure, edge emitting laser. [From Besomi et al., Electronics Letters, Vol. 20, pp. 417-419 (1984)]*

Note the increase in the lasing threshold current with increasing temperature. It is common to characterize the temperature dependence of the current threshold with a parameter T_0 by fitting data to the expression

$$I_{th}(T) = I_0 e^{\frac{T}{T_0}}.$$ *(Equation 7.1)*

The data of **Figure 7.4** give a T_0 of about 60°K. Typical values for long wavelength semiconductor lasers (λ_0 from 1.3 to 1.55 μm) are in the range of 50 to 70°K.

Also note the saturation of the output power at higher currents. The saturation is a result of laser heating that reduces the pumping efficiency of the device and the amount of pump current that is converted to optical output.

The L-I curve for a typical VCSEL is pictured in **Figure 7.5**. The VCSEL, with an InGaAs active region, has an output wavelength of approximately 0.9 μm. Note that the threshold pump current of just under 1 mA is lower than for typical edge emitting semiconductor lasers. Very low threshold currents are an advantage for VCSELs.

The output power for the VCSEL, approximately 1 mW, is also considerably smaller than for typical edge emitting semiconductor lasers. Generally, the output power for VCSELs is in the approximate range of 0.1 to 10 mW, however, VCSELs with multi-mW optical outputs usually operate in multiple lateral modes and, as a result, have outputs that are less spatially coherent.
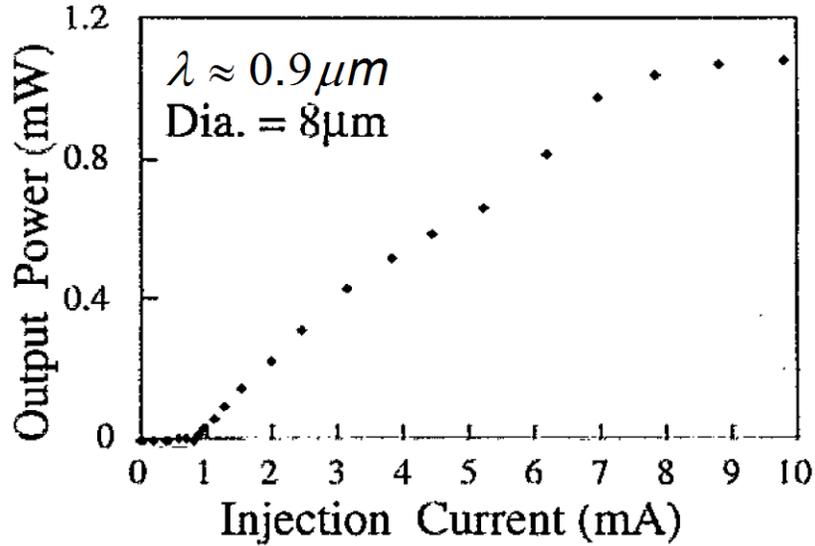
$\lambda \approx 0.9\,\mu m$
Dia. = 8μm

Figure 7.5: The L-I curve for an InGaAs VCSEL. [From Chang-Hasnain et al., Appl. Phys. Lett., Vol. 63, pp. 1307-1309 (1993)]

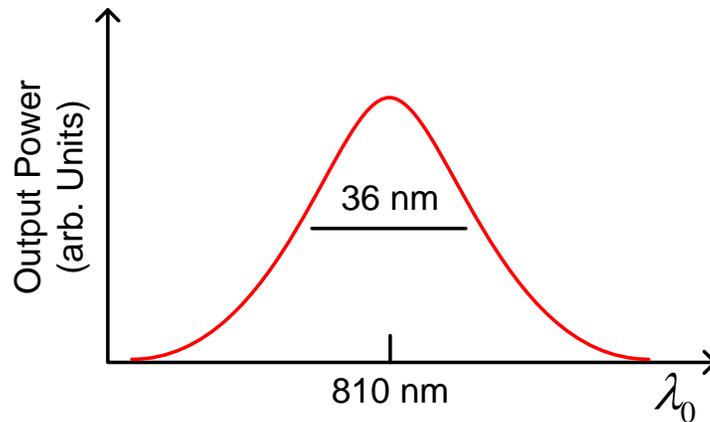## Spectral Properties

36 nm

810 nm

λ_0

Figure 7.6: The spectral output of a light emitting diode.

The spectral width of the output from an LED is the broadest of the semiconductor sources considered here. **Figure 7.6** is a sketch of a typical output for an LED that emits at 810 nm. The 36 nm width of the output is the full width at half maximum.
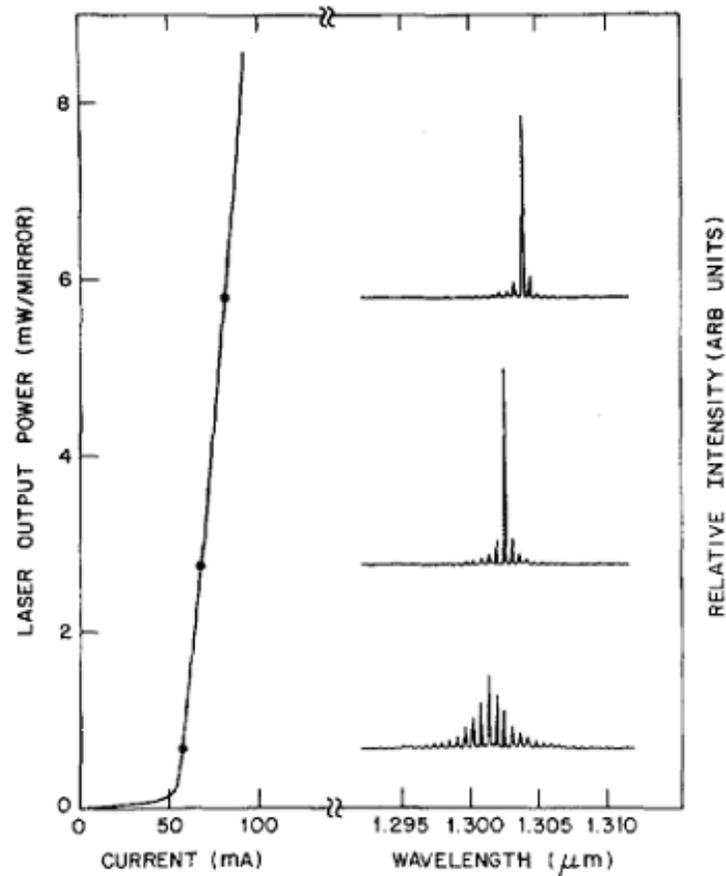
Figure 7.7*: Output spectra for a buried heterostructure Fabry-Perot type semiconductor laser. [From Nelson et al., J. Quantum Electron., Vol. QE-17, pp. 202-207 (1981)]*

The spectral output of a Fabry-Perot type semiconductor laser is considerably narrower than that of an LED. However, the spectra of a Fabry-Perot type laser consists of multiple longitudinal modes and can span several nanometers. Optical spectra for a buried heterostructure laser emitting at approximately 1.3 µm are pictured in **Figure 7.7**. Note that increase in the strength of the center mode relative to the side modes as the pump current is increased above threshold – a trend that is seen with most Fabry-Perot type lasers.

Frequency selective elements are used to force semiconductor lasers to operate in a single longitudinal mode. A common approach is to use a distributed Bragg reflector (**Figure 7.8**) to suppress all but a single longitudinal mode.
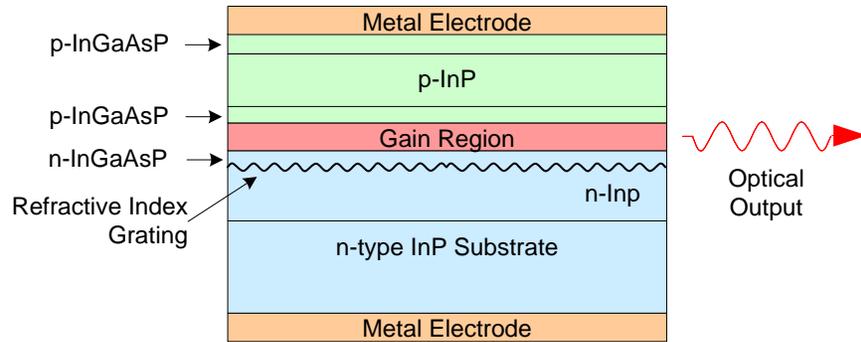
Figure 7.8: *A refractive index grating (distributed Bragg reflector) in a distributed feedback semiconductor laser interacts with light in the laser and suppresses all but one longitudinal mode.*

The spectral output for a distributed feedback laser at various current pumping levels is shown in **Figure 7.9**. The ratio of the center peak to the second highest peak is known as the "side mode suppression". The data show that the side mode suppression can be quite high (40 dB = 10,000).
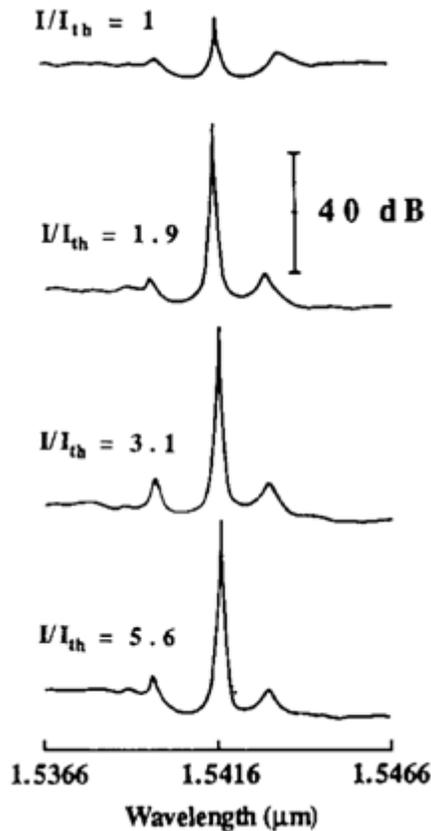

Figure 7.9: *Output spectra for a buried heterostructure, distributed feedback laser. [From Aoki et al., IEEE Photon Technol. Lett., Vol. 2, pp. 617-619 (1990)]*

VCSELs have similar spectral properties to those shown for the buried hetrostructure.

The theoretical value for the width of a single longitudinal mode is determined in the following way. The rate at which photons in a laser resonator are replaced by incoherent spontaneous emission is

$$\frac{d\phi}{dt} = \beta B n^2 V,$$

(Equation 7.2)

where ϕ is the total number of photons in the resonator, B is a constant that gives the rate of spontaneous emission, β gives the fraction of spontaneous emission that becomes part of the circulating laser beam and is called the spontaneous emission factor, n is the electron population density, and V is the volume of the gain region. This leads to a lifetime for coherent photons in the circulating beam of

$$\frac{1}{\tau_{ph}} = \frac{\frac{d\phi}{dt}}{\phi} = \frac{\beta B n^2 V}{\phi}.$$

(Equation 7.3)

The exponential decay of coherent photons in the resonator gives a Lorentzian profile for the frequency spectrum of the laser beam with a full width at half maximum of

$$\Delta \nu_L = \frac{1}{2}\frac{1}{2\pi\tau_{ph}} = \frac{\beta B n^2 V}{4\pi\phi}.$$

(Equation 7.4)

This is the famous Schawlow-Townes linewidth for a laser, with a factor of ½ added to because we are interested only in phase fluctuations contributed by spontaneous emission.

Actually, a modification must be made to the Schawlow-Townes formula in order to produce a correct expression for the linewidth in a semiconductor laser. Fluctuation in the carrier density n leads to a corresponding fluctuation in the laser gain, which in turn leads to fluctuation in the refractive index of the gain medium. An important quantity in this process is the linewidth enhancement factor given by

$$\overline{\alpha} = \frac{\Delta n_r'}{\Delta n_r''},$$

(Equation 7.5)

where $\Delta n_r'$ and $\Delta n_r''$ are the real and imaginary parts, respectively, of the refractive index for the gain medium. Typical values for the enhancement factor range from 2 to 10. To take into account fluctuations in refractive index we must modify the Schawlow-Townes formula to read

$$\Delta v_L = \frac{\beta B n^2 V}{4\pi\phi}\left(1+\overline{\alpha}^2\right).$$

When used to describe most types of lasers, the Schawlow-Townes expression gives a linewidth that is much larger than what is observe because laser linewidth is generally dominated by "technical" contributions (e.g. variations in cavity length due to thermal fluctuations). Semiconductor lasers are an exception. Their inherent structural stability and relatively large spontaneous emission rate mean that their linewidths approach the Schawlow-Townes limit.

Now let's take a look at some experimental laser linewidth data (**Figure 7.10**). Two distributed feedback lasers were examined. One had a relatively thick "bulk" layer of semiconductor for the active region. The active region of the second laser contained a series of very thin layers of semiconductor designed to trap electron and holes in "multiple quantum wells" (MQWs). Both showed a decrease in laser linewidth for increasing output power from smaller values up to about 10 mW. This is consistent with the Schawlow-Townes linewidth, which has the photon number ϕ in a denominator. The smaller linewidth for the MQW laser is attributed to a correspondingly smaller linewidth enhancement factor. The data for both lasers also show an increase in linewidth for output power that exceeds 10 mW that is believed to be due to 1 over f noise.
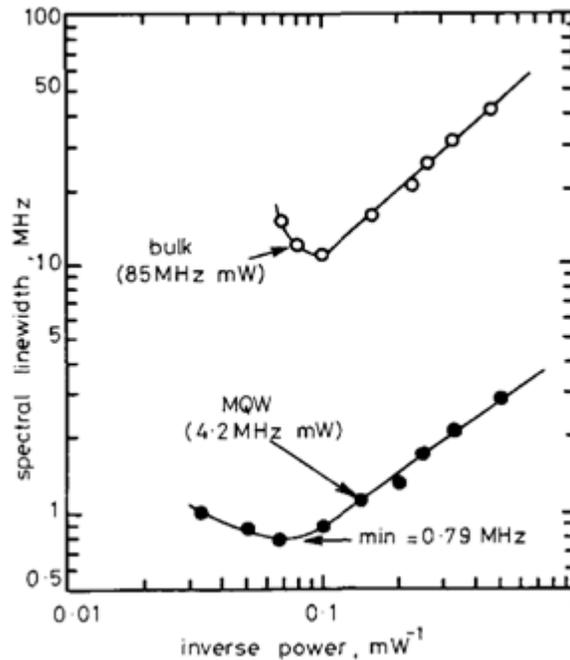

Figure 7.10: *Linewidth for the fundamental longitudinal mode of DFB lasers. [From Uomi et al., Electron. Lett. Vol. 26, pp. 52-53 (1990)]*

Relative Intensity Noise and Signal to Noise Ratio

The optical output of light emitting diodes and semiconductor laser is very stable. So much so that commercial data sheets rarely specify amplitude stability. The relative intensity noise (RIN) spectrum for an optical source is defined by

$$RIN\,[db/Hz] = 10 \cdot \log \frac{\left\langle P_n^2 \right\rangle}{\left\langle P \right\rangle^2 \cdot BW},$$

where $\sqrt{\left\langle P_n^2 \right\rangle}$ is the average noise power, $\left\langle P \right\rangle$ is the average power, and BW is the detection bandwidth. **Figure 7.11** is a sketch of a typical relative intensity noise (RIN) spectra for a semiconductor laser. Note the spectral peaks due to resonant "relaxation oscillations" in the laser resonator. Also note that the resonant peak is pushed to higher frequency at higher laser power.
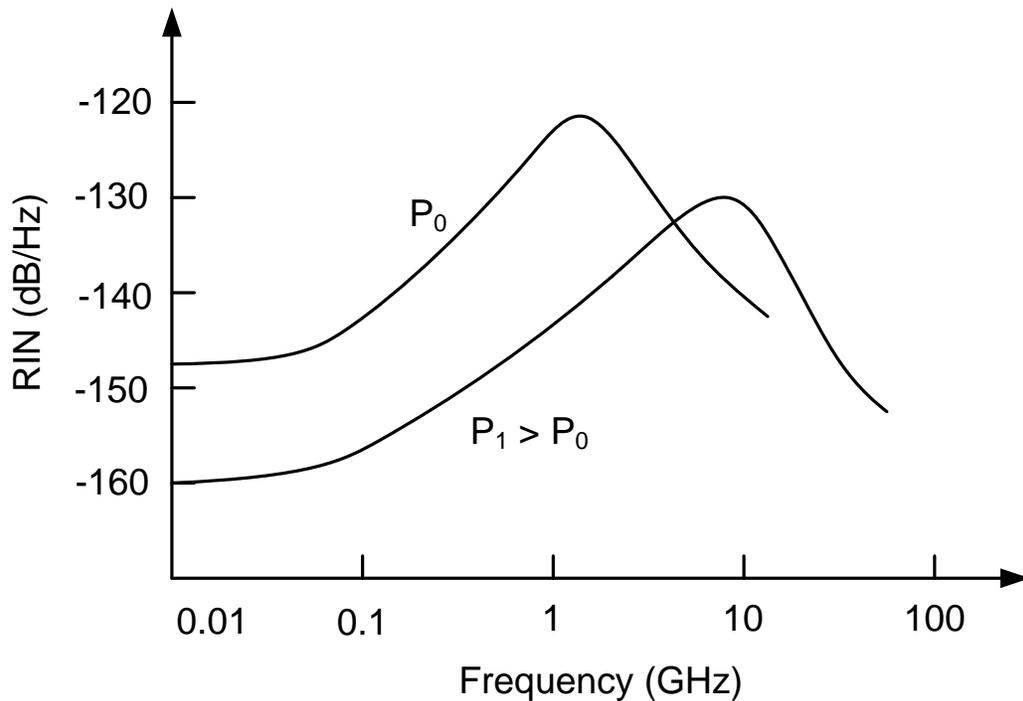

Figure 7.11: A sketch of relative intensity noise for a semiconductor laser at two powers.

To make the values in **Figure 7.11** more intuitive, we will calculate the signal to noise ratio if the RIN is -150 dB/Hz, the laser power is 1 mW, and the detector bandwidth is 100 MHz. In this case the noise power is

$$\langle P_N \rangle = \sqrt{\langle P_N^2 \rangle}$$

$$= \sqrt{10^{\frac{RIN}{10}} \cdot \langle P \rangle^2 \cdot BW} \qquad , \qquad \text{(Equation 7.8)}$$

$$= \sqrt{10^{-14} \left(10^{-3}W\right)^2 \cdot 10^8}$$

$$= 1\mu W$$

and the signal to noise ratio is

$$SNR = \frac{\langle P \rangle}{\langle P_N \rangle} = \frac{1mW}{1\mu W} = 1000 = 30 \; dB \cdot \qquad \text{(Equation 7.9)}$$

7.2 Output Modulation

Direct Modulation

Supplying a modulated current to the source can directly modulate the optical output of a semiconductor source. Directly modulated light emitting diodes can be used for data transmission at rates of up to approximately 100 Mbits/sec, limited by the lifetime of injected charge. The very broad spectral output of LEDs also limits their usefulness to transmission over distances of no more than a few kilometers as optical pulses tend to spread due to chromatic dispersion in optical fibers.
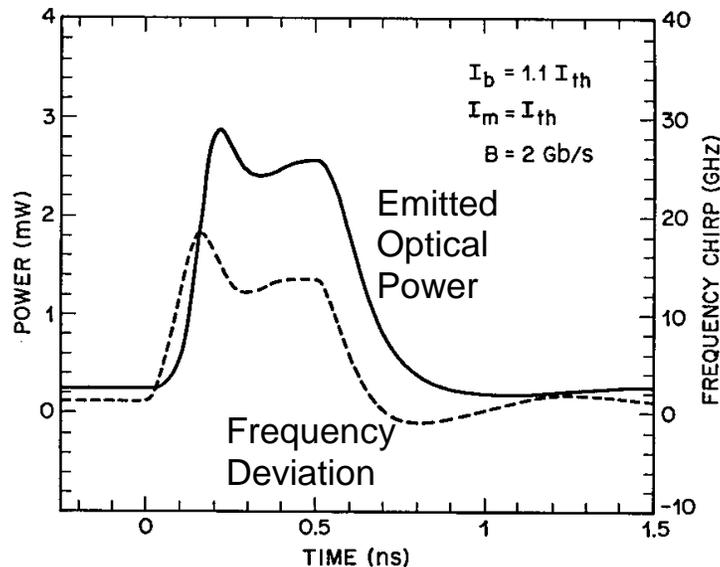

Figure 7.12: The calculated response of a semiconductor laser to a 500 psec rectangular current pulse, equivalent to a bit rate of 2 Gbits/sec. The laser is biased at 1.1 times the threshold current and the modulation current equals the threshold current. [From Fiber-Optic

Communication Systems, 2nd Edition, Govind P. Agrawal (John Wiley & Sons, New York, 1997) p. 116].

Single mode semiconductor lasers (such as DFB lasers) are the source of choice for direct modulation at high speeds and over long distances. The factors that limit modulation rate and transmission distance can be considered with the aid of **Figure 7.12**, which shows a simulation of the response of a semiconductor laser to a 500 picosecond rectangular current pulse. The solid curve is the simulated optical output. The pulse is slightly distorted, with sloped sides and ringing at the top of the pulse. Higher data rates (i.e. greater than 2 Gbits/sec) would mean shorter pulses, more significant distortion, and a possible loss of information in a data stream containing multiple pulses.

The dashed line in **Figure 7.12** displays the calculated frequency deviation during the pulse. The frequency deviation, or "chirp", is due to changes in the refractive index in the gain region of the laser that accompany the modulated gain coefficient. The linewidth enhancement factor, discussed in the previous section, gives a direct measure of the magnitude of these frequency excursions. In order to see how chirp limits the length of a fiber optic communication length, consider that the frequency excursion for the 500 psec pulse in **Figure 7.12** is approximately 19 GHz – equal to 0.152 nm for a laser operating at 1550 nm. A typical value for group velocity dispersion in an optical fiber at 1550 nm is 16 ps/(km-nm) so the pulse spreading is

$$\frac{\delta\left(\Delta\tau_p\right)}{L}\text{[psec/km]} = \left(0.152nm\right)\left(16\frac{p\sec}{km\cdot nm}\right) = 2.44\times\frac{p\sec}{km}. \qquad \textit{(Equation 7.10)}$$

We can assume that pulse spreading is a significant problem when

$$\delta\left(\Delta\tau_p\right) = 0.7\cdot\Delta\tau_p = 350\,p\sec. \qquad \textit{(Equation 7.11)}$$

Thus the maximum length of an optical fiber span is

$$L_{\max} \approx \frac{350\,p\sec}{2.44\frac{p\sec}{km}} = 143\ km. \qquad \textit{(Equation 7.12)}$$

External Modulation and the Pockels Effect

Optical communications over long distance with a data rate of 10 Gbits/sec or higher typically use a CW (continuous wave) single mode laser together with an external optical modulator as shown in **Figure 7.13**. This configuration circumvents some of the issues discussed in the previous section, particularly the limit on optical span length imposed by laser chirp.
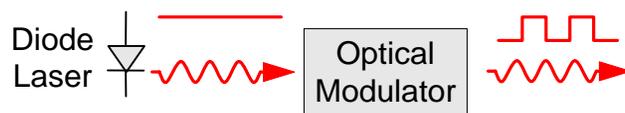
Figure 7.13: *A CW laser with an external optical modulator.*

The optical modulator most widely used for high-speed, long-haul optical communication is made with a crystal of lithium niobate (LiNbO$_3$). The physical mechanism for optical modulation is the linear electrooptic effect, also known as the Pockels effect after the German physicist who first described the effect in 1893. To understand the linear electrooptic effect in lithium niobate, an optically anisotropic material, we must introduce the concept of the index ellipsoid.

The index ellipsoid is described by the equation

$$\frac{x'^2}{n_{x'}^2} + \frac{y'^2}{n_{y'}^2} + \frac{z'^2}{n_{z'}^2} = 1, \qquad \textit{(Equation 7.13)}$$

where x′, y′, and z′ are distances along the principal axes of the crystal, and by the equation

$$\left(\frac{1}{n^2}\right)_1 x^2 + \left(\frac{1}{n^2}\right)_2 y^2 + \left(\frac{1}{n^2}\right)_3 z^2$$
$$+ \left(\frac{1}{n^2}\right)_4 2yz + \left(\frac{1}{n^2}\right)_5 2xz + \left(\frac{1}{n^2}\right)_6 2xy = 1 \qquad \textit{(Equation 7.14)}$$

for an arbitrary collection of Cartesian axes.

Now let's see how to use the index ellipsoid, working with the diagram in **Figure 7.14**, for which the x, y, and z axes coincide with the principal axes. Consider a electromagnetic plane wave with a wavevector $\vec{k}$. A plane through the origin perpendicular to $\vec{k}$ cuts the ellipsoid in an ellipse that is indicated with a shaded interior. There are two normal modes for this wave. The first is linearly polarized along the minor axis of the ellipse and experiences a refractive index equal to
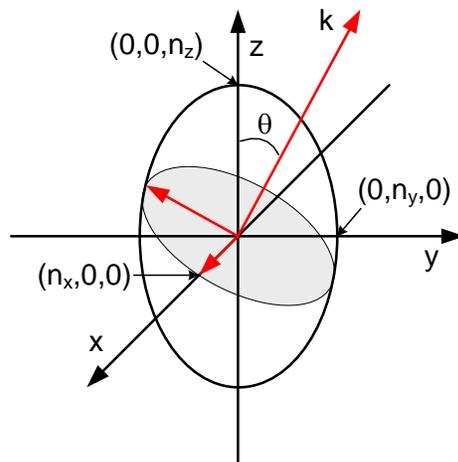
Figure 7.14: *The index ellipsoid.*

the half width of the minor axis (i.e. the distance from the origin to the ellipsoid along the direction of polarization). The second normal mode is linearly polarized along the major axis of the ellipse and experiences a refractive index equal to the half width of the major axis. Waves polarized along other directions do not propagate as linearly polarized waves but as elliptically polarized combinations of the normal modes.

Now consider the special case where $\vec{k}$ lies in the y-z plane so that one of the normal modes is polarized along the x axis. The index ellipse for this case is pictured in **Figure 7.15**. There will always be a normal mode along the x axis, regardless of the angle θ between $\vec{k}$ and the z axis, and these modes all experience a refractive index $n_o = n_x$ that is called the ordinary index. The refractive index for the second normal mode, called the extraordinary wave, has θ dependence given by

$$n_{ext}(\theta) = \sqrt{\frac{n_y^2 n_e^2}{n_e^2 \cos^2\theta + n_y^2 \sin^2\theta}}, \qquad \textit{(Equation 7.15)}$$

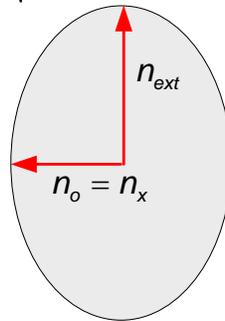and varies from n_y to n_e, where $n_e = n_z$ is called the extraordinary index.

Figure 7.15: *The index ellipse*

For lithium niobate $n_x = n_y$, which makes it a "uniaxial" crystal and means that there is always an ordinary mode regardless of the direction of the wavevector $\vec{k}$. The values for n_0 and n_e for lithium niobate are 1.8830 and 1.7367, respectively, at a wavelength λ_0=632 nm. All waves propagating in the z direction are ordinary and the z axis is also called the optical axis.

Linear Electrooptic Effect

An electric field $\vec{E} = (E_x, E_y, E_z)$ applied to a crystal can distort the index ellipsoid (this DC or quasi-DC field is not to be confused with the optical field). The changes can be described in the most general way with the matrix expression

$$
\begin{bmatrix}
\Delta\left(\dfrac{1}{n^2}\right)_1 \\[6pt]
\Delta\left(\dfrac{1}{n^2}\right)_2 \\[6pt]
\Delta\left(\dfrac{1}{n^2}\right)_3 \\[6pt]
\Delta\left(\dfrac{1}{n^2}\right)_4 \\[6pt]
\Delta\left(\dfrac{1}{n^2}\right)_5 \\[6pt]
\Delta\left(\dfrac{1}{n^2}\right)_6
\end{bmatrix}
=
\begin{bmatrix}
r_{11} & r_{12} & r_{13} \\
r_{21} & r_{22} & r_{23} \\
r_{31} & r_{32} & r_{33} \\
r_{41} & r_{42} & r_{43} \\
r_{51} & r_{52} & r_{53} \\
r_{61} & r_{62} & r_{63}
\end{bmatrix}
\cdot
\begin{bmatrix}
E_x \\
E_y \\
E_z
\end{bmatrix},
\qquad \textit{(Equation 7.16)}
$$

where the matrix of r values is called the electrooptic tensor. This equation looks complicated but in most cases crystal symmetry greatly simplifies the electrooptic tensor. The electrooptic tensor for lithium niobate is

$$
r =
\begin{bmatrix}
0 & -r_{22} & r_{13} \\
0 & r_{22} & r_{13} \\
0 & 0 & r_{33} \\
0 & r_{51} & 0 \\
r_{51} & 0 & 0 \\
-r_{22} & 0 & 0
\end{bmatrix},
\qquad \textit{(Equation 7.17)}
$$

where the values of the components of the electrooptic tensor are given in Table 1.

Table 1. Components for the electrooptic tensor for LiNbO$_3$.

Component	Value [10^{-12} meter/volt]
r_{13}	9.6
r_{22}	6.8
r_{33}	30.9

r_{51}	32.6

Of the two larger components, only r_{33} can be used to generate a simple change in the refractive index experienced by a linearly polarized wave, and most lithium niobate electrooptic modulators are designed to use r_{33}. The change in the index ellipsoid for a lithium niobate crystal with an electric field applied along the optical (z) axis is shown in **Figure 7.16**. The distortions are

$$n_0(E_z) = n_0 - \frac{1}{2}n_o^2 r_{13} E_z,$$ *(Equation 7.18)*

and

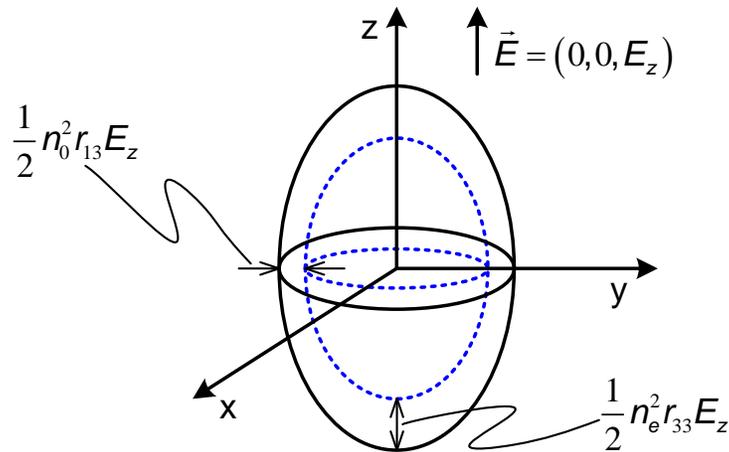$$n_e(E_z) = n_e - \frac{1}{2}n_o^2 r_{33} E_z.$$ *(Equation 7.19)*

Figure 7.16: *The change in the index ellipsoid for LiNb$_{O3}$ for an electric field applied along the z axis.*

Electrooptic Modulation

A lithium niobate electrooptic modulator is illustrated in **Figure 7.17**. The crystal is "x-cut", which means that the x axis of the crystal is perpendicular to the top surface of the device. Light is confined to optical waveguides in the crystal that are fabricated by titanium indiffusion or a process known as proton exchange. Optical input, polarized along the z axis of the crystal, is split between two arms of the waveguide. The optical fields in the two arms of the device will undergo different phase shifts depending on the refractive index each experiences. The two fields are recombined at the device output and the interference between the beams yields a modulated optical output from the device. This type of device is called a Mach-Zender-type optical interferometer.

Specifically, voltage applied to the electrodes generates an electric field along the z axis in the waveguides, modifies n_e (the refractive index experienced by the guided waves), and modifies the phase of the light as it travels the length of the interferometer's arms. The electric field is in opposite directions in the two arms, so the refractive index is raised in one arm and lowered in the other. The upper portion of **Figure 7.17** pictures the situation where an applied voltage produces light that is in phase and interferes constructively where the interferometer's arms recombine. In this case the optical input appears at the modulator's output. As pictured in the lower portion of **Figure 7.17**, an applied voltage produces light that is out of phase at the end of the interferometer's arms. This light couples into radiation modes in the output waveguide that leaks out of the sides of the waveguide. In this case optical input does not appear at the output.
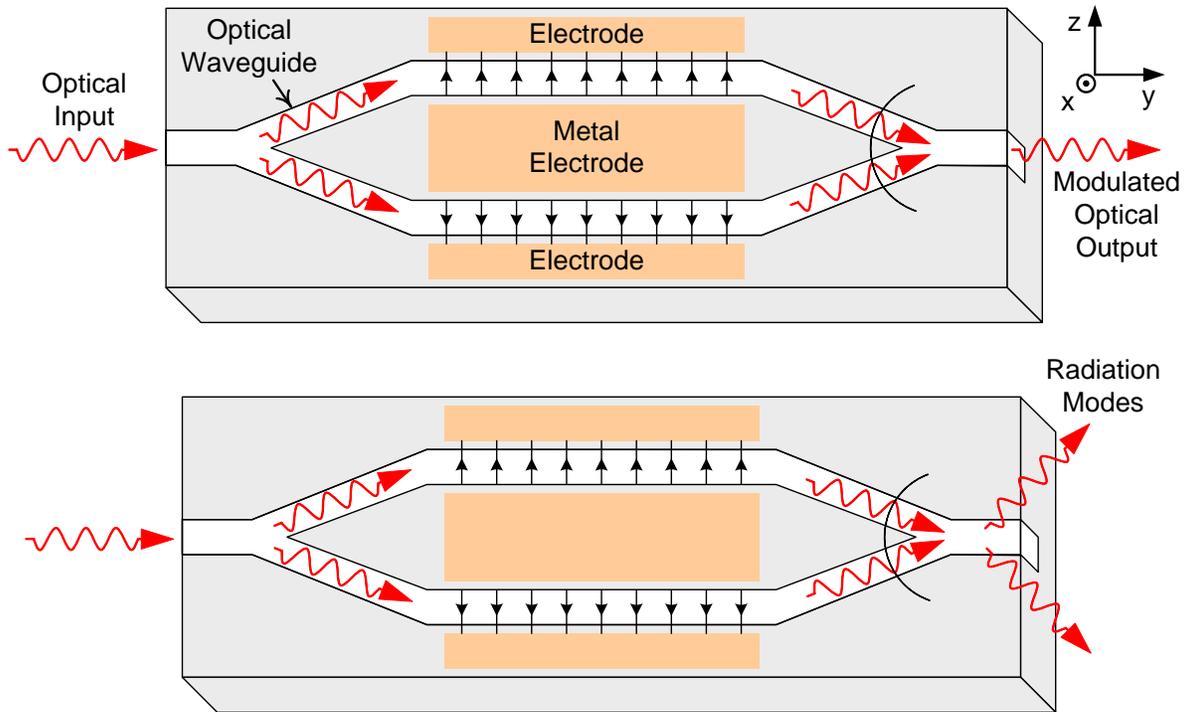

Figure 7.17: A optical amplitude modulator with a Mach-Zender configuration.

Lithium niobate optical modulators such as the one pictured in **Figure 7.17** introduce very little chirp into an optical signal and can be used to transmit optical data over 100's of kilometers at data rates of up to 40 Gbits/sec.

7.3 Transmitter Design

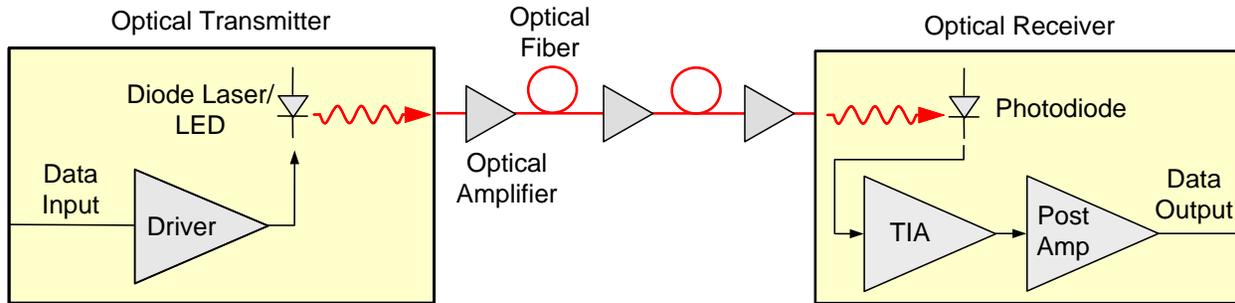*Optical Data Link with a Directly Modulated Source*

Figure 7.18: *An optical data link with an optical transmitter that uses a directly modulated light emitting diode or semiconductor laser.*

An optical transmitter is the front end of an optical data link as illustrated in **Figure 7.18**. Data are in the electrical domain when they reach the transmitter module, where they are input for an electrical driver circuit. The driver provides a time varying current to a light emitting diode (LED) or semiconductor laser in order to encode the electrical data onto the optical output of the LED or laser. LED's are simpler and less expensive than laser diodes, but a laser diode should be used for data transmission at rates that exceed about 200 Mbits/sec.

The optical signal leaves the transmitter in optical fiber for transmission to a remote location. For long data links, optical amplifiers are used to compensate for optical attenuation of the data signal in the fiber. Data are converted into an electrical signal at the receiving end of the data link using a photodiode connected to a transimpedance amplifier (TIA) connected to a second limiting amplifier or automatic gain control amplifier (post amplifier).

Figure 7.19 shows a somewhat more detailed picture of an optical transmitter with a laser source. Electrical data input is regenerated, i.e. retimed and reshaped. This is usually accomplished with a flip-flop circuit that is set by external clock signals. The regenerated electrical data stream is input to a modulation circuit, and the time varying electrical current output is used to modulate the laser. The laser is biased just below threshold with a separate bias control circuit. The temperature of the optical transmitter is stabilized using a thermistor to monitor temperature and a thermoelectric cooler to adjust temperature to a specified value.
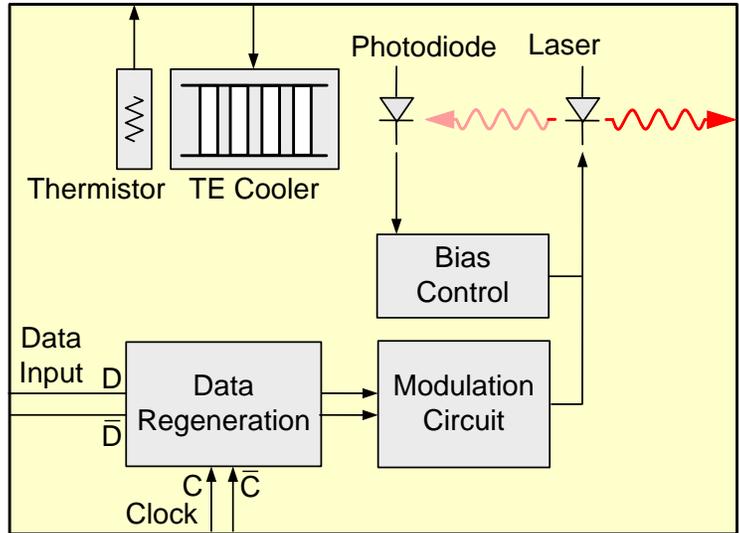
Figure 7.19: *An optical transmitter.*

Despite temperature stabilization, laser threshold current can vary with time, so adjustment of the laser bias current is required. A photodiode is used to monitor the average power emitted from the back side of the laser source. The bias control circuit adjusts the DC laser bias current in order to maintain a constant signal from the photodiode and a specified optical output from the laser.

Optical Data Link with an External Optical Modulator

At data rates that exceed 2.5 Gbits/sec, a directly modulated laser exhibits nonlinear effects (chirp) that can distort an optical data signal. For this reason, it is common at very high data rates to use an optical transmitter with a combination of a CW (continuous wave) laser and an optical modulator as shown in **Figure 7.20**. Data is encoded on light from the semiconductor laser as it passes through the optical modulator. This type of transmitter can be used to send data at rates of up to 40 Gbits/sec.
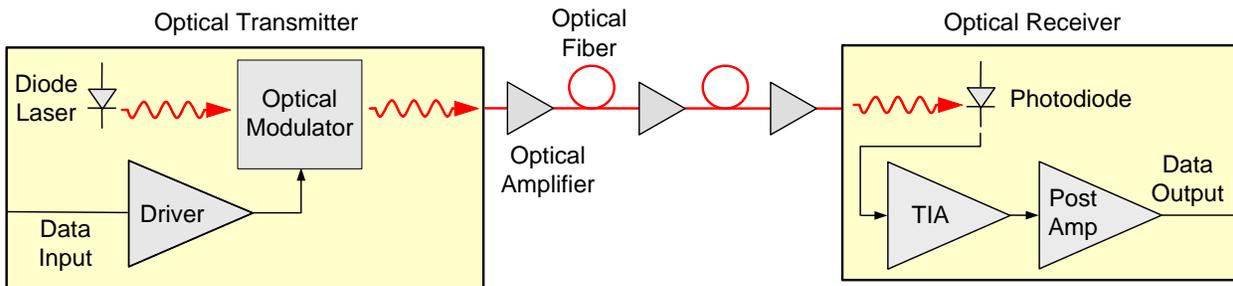

Figure 7.20: *An optical data link with an optical transmitter that uses a CW diode laser and a separate optical modulator.*

Transmitter Circuitry

The modulation circuit of **Figure 7.19** can be implemented with the components shown in **Figure 7.21**. The current source sinks current through the resistor R or the laser/optical modulator load. When D is high, transistor Q_1 turns on, $\overline{D}$ turns transistor Q_2 off, and current flows through the resistor R. When D is low, Q_1 is off, Q_2 is on, and current flows through the laser/optical modulator load.
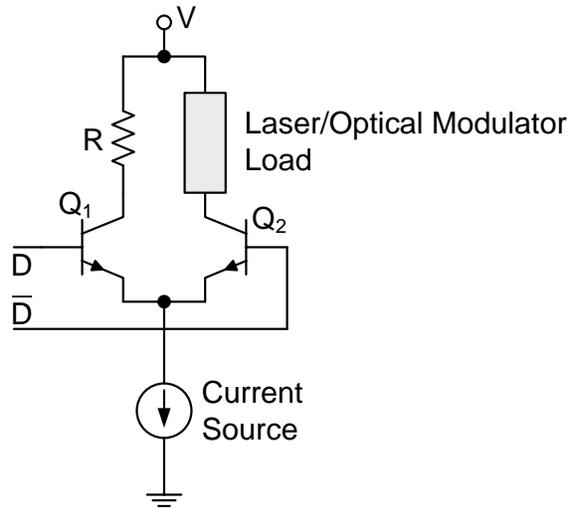

Figure 7.21: Current steering circuitry to modulate a semiconductor laser or optical modulator.

Frequently it is necessary to provide additional predriver circuitry that serves as an interface between the regenerating flip flop and the current steering circuitry of **Figure 7.21**, conditioning data signals before they arrive at transistors Q_1 and Q_2. This simple addition is pictured in **Figure 7.22.**
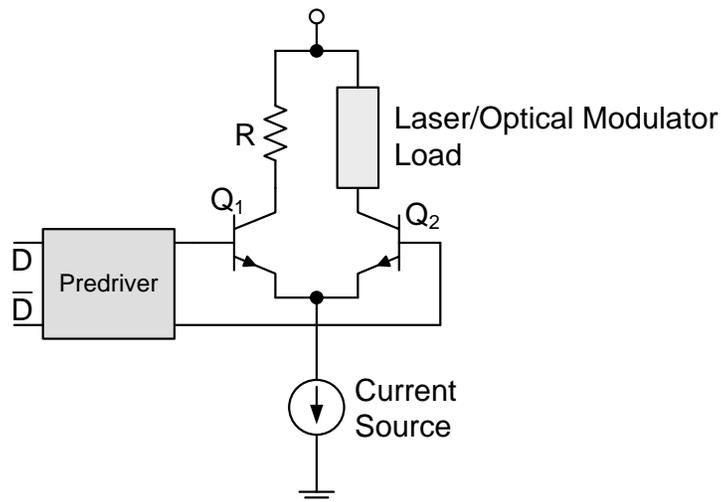

Figure 7.22: Modulation circuitry with an additional predriver.

Laser/Optical Modulator Loads

A semiconductor laser can be DC coupled to a modulation circuit using the simple resistor/laser combination shown in **Figure 7.23a**. The resistor dampens current oscillations due to parasitic inductances in the circuitry.
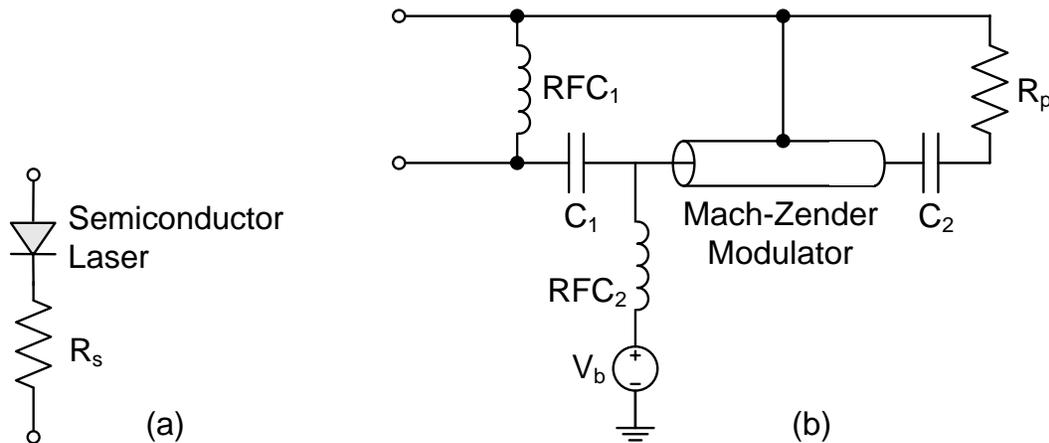

Figure 7.23: *Loads for the modulator circuitry of Figures 7.21 and 7.22. (a) A DC coupled semiconductor laser and (b) An AC coupled optical modulator.*

An optical modulator can be coupled to a modulation circuit using the circuit in **Figure 7.23b.** From an electrical viewpoint the optical modulator is a transmission line. The modulation circuit is AC coupled to the optical modulator with the RF choke (inductor) RFC_1 and the capacitor C_1. The optical modulator is biased by the supply V_b though a bias T that is comprised of C_1 and RFC_2. The modulation voltage is given by the product of the modulation current I_m and the termination resistor R_p. The capacitor C_2 blocks DC current through the optical modulator.

From an electrical viewpoint, a push-pull (dual drive) type optical modulator is a pair of transmission lines. The modulation circuitry for a push-pull modulator must drive a pair of loads, each similar to **Figure 7.23b**. Each load is driven by a separate arm of the current steering circuitry.

Laser Bias Control

Figure 7.24 shows an implementation of laser bias control. Light from the back side of the semiconductor laser is directed towards a photodiode that is used to monitor the laser output. A resistor/capacitor pair (R and C) convert current from the photodiode into a DC voltage that is one of the inputs to an operational amplifier. The voltage is compared with a reference voltage V_{REF} that is applied to the other op amp input. Output from the differential amplifier drives an adjustable current source that provides the bias to the semiconductor laser.
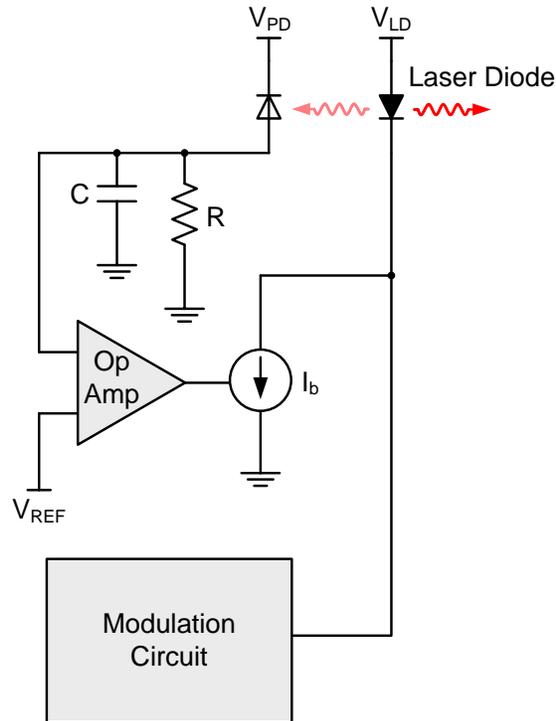
Figure 7.24: *A circuit for laser bias control.*

Packaging

An example of an optical transmitter package is illustrated in **Figure 7.25**. The photodiode, thermistor, and thermoelectric cooler have been discussed in previous sections. An anti-reflection coated lens collimates the divergent optical output of the semiconductor laser. An optical isolator prevents reflected light from other parts of the optical system from reaching the laser. Without isolation, reflected light can be a significant source of optical noise. A hermetically sealed enclosure (not shown in the figure) prevents moisture and other environmental contaminants from reaching the sensitive optical components. Light passes through a window in the enclosure to be focused into an optical fiber.
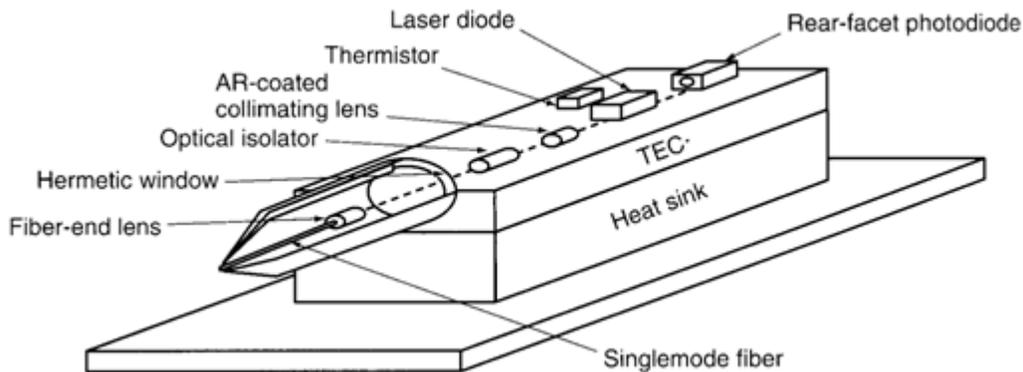
Figure 7.25: *A packaged optical transmitter. [From Fiber-Optic Communica-tions Technology, Mynbaev and Scheiner, (Prentice Hall, Upper Saddle Back River, NJ, 2001) p. 410]*

Reliability

Transmitter reliability is commonly characterized by two statistical measures - failures in time (FIT) and mean time to failure (MTTF). FIT is the number of failures per billion hours of operation. MTTF is the average time before a device fails. In optical transmitters the semiconductor laser is what most often fails first. Typical FIT and MTTF are given in **Table 1**.

Table 1. Temperature dependence of FIT and MTTF for optical trans-mitters. [From *Fiber-Optic Communications Technology*, Mynbaev and Scheiner, (Prentice Hall, Upper Saddle Back River, NJ, 2001) p. 412].

Temperature	FIT	MTTF
25°C	294	2.4×10^6 hours (274 years)
50°C	1456	0.69×10^6 hours (78 years)

Note the relatively small number of failures in time and very long mean time to failure. The values make direct measurement of FIT and MTTF impractical. However, the increase of FIT and decrease of MTTF with increasing temperature is the key to estimating their values. "Accelerated" testing is carried out by measuring FIT and MTTF at an elevated temperature and extrapolating to lower temperature.